

AD A098823

DTIC FILE COPY

OFFICE OF NAVAL RESEARCH

Contract N00014-79-0622

Task No. NR 056-729

TECHNICAL REPORT NO. 3

Noble Gas Condensation in Controlled-Expansion Beam Sources

by

S. S. Kim, D. C. Shi and G. D. Stein

Prepared for Publication

in

Rarefied Gas Dynamics, AIAA

Northwestern University  
Departments of Mechanical and Nuclear Engineering,  
Chemistry, and Physics  
Evanston, Illinois 60201

April, 1981

Reproduction in whole or in part is permitted for any purpose of the United States Government

This document has been approved for public release and sale; its distribution is unlimited

12 SC

101 Saig Soo / Kim  
Dian Cheng / Shi  
Gilbert D. / Stein

MAY 13 1981

(9) Mechanical Dept.

SECURITY CLASSIFICATION OF THIS PAGE (When Data Entered)		REPORT DOCUMENTATION PAGE		READ INSTRUCTIONS BEFORE COMPLETING FORM	
1. REPORT NUMBER	2. GOVT ACCESSION NO.	3. REPORT NUMBER	4. REPORT NUMBER	5. REPORT NUMBER	6. REPORT NUMBER
Technical Report No. 3	AD-A098823				
7. TITLE (and Subtitle)		8. TYPE OF REPORT & PERIOD COVERED			
Noble Gas Condensation in Controlled-Expansion Beam Sources		Interim			
9. AUTHOR(s)		10. PERFORMING ORG. REPORT NUMBER			
S. S. Kim, D. C. Shi and G. D. Stein		H00014-79-0622			
11. PERFORMING ORGANIZATION NAME AND ADDRESS		12. PROGRAM ELEMENT, PROJECT, TASK AREA & WORK UNIT NUMBERS			
Northwestern University, Departments of Mechanical and Nuclear Engineering, Chemistry, and Physics, Evanston, Illinois 60201		NR 056-729			
13. CONTROLLING OFFICE NAME AND ADDRESS		14. SECURITY CLASS. (of this report)			
Office of Naval Research Chemistry Program Code 472 Arlington, Virginia 22217		Unclassified			
15. DISTRIBUTION STATEMENT (of this Report)		16. SECURITY CLASS. (of this page)			
OMR, Chicago 536 S. Clark Street Chicago, Illinois 60605		Unclassified			
17. DISTRIBUTION STATEMENT (of this Report)					
Distribution of this document has been approved for public release and sale; its distribution is unlimited.					
18. DISTRIBUTION STATEMENT (of this Report)					
15) N00014-79-C-0622					
19. SUPPLEMENTARY NOTES					
Prepared for publication in "Rarefied Gas Dynamics" AIAA, NY, 1981					
20. KEY WORDS (Continue on reverse side if necessary and identify by block number)					
Clusters, Nucleation, Laval nozzles, Gasdynamics, Electron diffraction, Ar, Kr, Xe					
21. ABSTRACT (Continue on reverse side if necessary and identify by block number)					
Over the past several years an investigation into the gasdynamic and nucleation properties of very small Laval nozzles has been undertaken in our laboratory due to their great potential use as sources for cluster beams. A series of nozzles designed specifically for helium carrier gas expansions has been tested in our molecular beam apparatus and used to study the condensation of the noble gases, Ar, Kr, and Xe. The goal of producing cluster beams with densities high enough to carry out high energy electron diffraction experiments has been attained for these gases with mean cluster					

DD FORM 1 JAN 79 1473

SECURITY CLASSIFICATION OF THIS PAGE (When Data Entered)

145-760

81 5 12 037

712

20. sizes in the range of 100-400 atoms per cluster. The onset of nucleation appears to correlate with the product of nozzle diameter, starting pressure, and atomic potential well depth, i.e.,  $p_0 D_0$  e/k.

To Appear in  
Rarefied Gas Dynamics  
AIAA, N.Y. 1981  
(RGD Symposium)  
U. Virginia, 1980

# NOBLE GAS CONDENSATION IN CONTROLLED-EXPANSION BEAM SOURCES

Seng Soo Kim,<sup>\*</sup> Dian Cheng Shi,<sup>†</sup> and Gilbert D. Stein<sup>‡</sup>  
Northwestern University, Evanston, Ill.

## Abstract

Over the past several years an investigation into the gas-dynamic and nucleation properties of very small Laval nozzles has been undertaken in our laboratory due to their great potential use as sources for cluster beams. A series of nozzles designed specifically for helium carrier gas expansions has been tested in our molecular beam apparatus and used to study the condensation of the noble gases, Ar, Kr, and Xe. The goal of producing cluster beams with densities high enough to carry out high energy electron diffraction experiments has been attained for these gases with mean cluster sizes in the range of 100-400 atoms per cluster. The onset of nucleation appears to correlate with the product of nozzle diameter, starting pressure, and atomic potential well depth, i.e.,  $p_0 D_0$  e/k.

## Introduction

It is well known that supersonic nozzles can have their contours designed to control, within limits, the rate of expansion and that they can be very much more effective in nucleating a particular gas than uncontrolled, free-jet<sup>1,2</sup>

Presented as Paper 145 at the Twelfth International Symposium on Rarefied Gas Dynamics, Charlottesville, Va., July 7-12, 1980. Copyright American Institute of Aeronautics and Astronautics, Inc., 1980. All rights reserved.

<sup>\*</sup>Gas Dynamics Laboratory, Department of Mechanical and Nuclear Engineering.

<sup>†</sup>Gas Dynamics Laboratory, Department of Mechanical and Nuclear Engineering. On leave from the Institute of Electronics Academia Sinica, People's Republic of China.

<sup>‡</sup>Gas Dynamics Laboratory, Department of Mechanical and Nuclear Engineering.

<sup>1</sup>An orifice or a converging-only nozzle both of which have their entire supersonic flow regimes as free-jets will be defined here as "free-jet" sources. The nozzle sources described in this paper are of the Laval type with supersonic flow in the nozzle before exiting as a free-jet.

Accession For	NTIS GRA&I	Unannounced	Justification
	DTIC TAB		
BY	Distribution/	Availability Codes	Dist. and/or

-2-

expansions having the same throat diameter. 1-4 Nozzles made of varying throat diameter, exit diameter, and nozzle length have been built and tested. They have been instrumented so that the following data can be obtained: stagnation pressure  $P_0$  and temperature  $T_0$ , nozzle exit static pressure  $P_1$ , pitot pressure measurements  $P_{02}$  near the nozzle exit, and pitot traverses parallel and normal to the flow direction.

The experimental arrangement is shown in Fig. 1a. The nozzle source is mounted with x-y-z motion capability and is shown with a diverging Level-type nozzle installed. If impact pressure measurements are to be made, the skimmer 5 is removed and a probe and pressure transducer are mounted so as to separate the first and second pumping chambers. Replacement of the skimmer re-establishes the standard molecular beam configuration. The cluster beam is crossed by a 40 keV electron beam for diffraction studies and Debye-Scherrer patterns are taken with a single-channel, electron-scintillator, photon counting detection system using phase-sensitive detection and a chopped molecular beam.

The contours for the nozzles used in this work are shown in Fig. 1b. The throat diameters vary from 0.05 to 0.1 mm, and exit diameters range from 2 to 5 mm. The nozzles are diverging with the minimum diameter at the entrance. The subsonic flow ahead of the entrance is not important for the nucleation process. Their contours have been measured and fitted to tenth order polynomials as shown in Table I. Nozzle 4 has the smallest divergence angle ( $<10^\circ$  total included angle) and is longer than the other nozzles. The noble gas experiments discussed here were obtained using Nozzles 11, 12 and 13. They were designed to determine the effect of throat diameter  $D_0$  and nozzle contour on their performance as cluster sources. Nozzles 12 and 13 have the same contour except near the nozzle entrance. Nozzle 11 diverges more rapidly than 12 and 13 near the inlet.

\*Pitot pressure is defined as the impact pressure and they are used here interchangeably.

# Gasdynamics Measurements

Extensive gasdynamic measurements using a variety of gases and gas mixtures reveal that a large fraction of the nozzle flow lies within the nozzle boundary layer with some viscous dissipation occurring all the way to the centerline. Thus, in order to correctly determine the local Mach number at any point in the nozzle, one must measure both static and impact pressure. The only point where both pressures are measured in this work is at the nozzle exit. The Mach number is obtained using the so-called Rayleigh supersonic pitot equation,

$$\frac{P_1}{P_{02}} = \left( \frac{2\gamma}{\gamma+1} M^2 - \frac{\gamma-1}{\gamma+1} \right)^{\frac{\gamma-1}{\gamma}} \left( \frac{\gamma+1}{2} M^2 \right)^{\frac{\gamma}{\gamma-1}} \quad (1)$$

where  $\gamma$  is the local value of the specific heat ratio. The exit Mach number  $M_0$  is shown in Fig. 2 for several gas mixtures, all of which are for 6 mole % of the condensable species in a helium carrier gas ( $X_0 = 0.06$ ). This Mach number is seen to increase monotonically with  $P_{02}$  to values as high as 10. The three solid curves are for Nozzle 12 with the different condensable species. For  $P_{02} < 4$  bar, the Mach numbers are nearly the same, but increase with molecular mass, i.e., from Ar to Kr to Xe. Above 4 bar the curves reverse, with Ar having the highest Mach number for any given  $P_{02}$ . For Xe, a comparison for the three nozzles, 11-13, is shown. Nozzle 12 gives the highest Mach number for a given  $P_{02}$  and Nozzle 11 (same throat size but more rapid expansion) is second highest. Nozzle 13 (same contour as 12 but smaller entrance diameter  $D_0$ ) exhibits the lowest Mach numbers.

With the system arranged in its molecular beam configuration, beam intensities were measured using an ionization gauge (IG in Fig. 1). The nozzle-to-skimmer distance,  $x_g$ , was varied to determine its effect on beam intensity. Pure argon expansions are shown in Fig. 3. Note that intensity variations with  $x_g/D_0$  are not large. There is an interesting variation in  $I_0$ , the beam intensity proceeding from a downstream peak location to a double peak to an upstream peak as  $P_{02}$  is increased. This behavior is similar to some previous free jet cluster source data.<sup>6,7</sup> All beam experiments now to be described were carried out with  $x_g = 2.5$  mm. This spacing gives a value of  $x_g/D_0 \approx 0.5$  for Nozzle 13, which is optimum for the high  $P_{02}$  beams as seen in Fig. 3. Since the exit diameter of Nozzles 11-13 are nearly equal,  $x_g/D_0 \approx 0.5$  for all of them and their beam intensities are near their maximum value.

Although Laval nozzles are much more efficient cluster sources than free-jets for most flows, care must be taken in their design or they can actually produce beam intensities lower than these latter sources. Consider for example the expansion of  $\text{SF}_6$  ( $X_0 = 0.125$ ) through Nozzle 4 shown in Fig. 4. When the  $\text{SF}_6$  is expanded in an argon carrier gas, the beam intensity increases dramatically near  $P_0 = 2.5$  bar due to clustering. However, for helium carrier gas (same specific heat ratio  $\gamma$ ) the beam intensities remain quite low even out to  $P_0 = 8$  bar, as typically seen with free-jet sources. Thus this nozzle is of little use for helium carrier gas, condensation experiments with  $T_0$  near room temperature.

Because a high  $\gamma$  carrier gas is required for condensation of a low  $\gamma$  gas in an adiabatic expansion, and because the Laval nozzles control the rate of expansion but cannot limit the maximum Mach number in these expansions, He is desirable since it is unlikely to supersaturate and thus will not form condensable carrier gas clusters. The use of pure condensable gas expansions is also an option, provided  $\gamma$  is not too near unity, but such use does not allow the possibilities for controlling the cluster size distribution or temperature that are potentially available through the use of a carrier gas. In addition there is the problem of the high cost of some pure gases such as Xe.

There are, however, a number of problems using He rather than other commonly used carrier gases such as Ar or  $\text{N}_2$ . For a given nozzle,  $P_0$  and  $T_0$  boundary layer effects are more severe for He due to its higher kinematic viscosity. There is also a problem with the high vacuum diffusion pumps (i.e., for nozzles with  $D_0 > 0.1$  mm pressure fluctuations of an order of magnitude or more occurred in the second and third stage pumping chambers when  $P_0 > 2$  bar.) Thus in order to operate at sufficiently high  $P_0$  for cluster beam generation, it is necessary to decrease the nozzle throat size below 0.1 mm. This exacerbates the problem of helium boundary layer growth. As a result of these criteria and prior experience with nozzles having long, small divergence inlets, e.g., Nozzle 4, several shorter nozzles that diverge more rapidly have been constructed.

### Nucleation

Measured molecular beam intensities for He-carried Ar, Kr, and Xe with  $X_0 = 0.06$  are shown in Fig. 5 for Nozzle 12 and  $T_0 = 295$ . As one might expect, condensation occurs in the order Xe, Kr, and Ar as  $P_0$  is increased. All the molecular beam intensity data are given in fixed, arbitrary units (but with the same a.u. in Figs. 3-7) with 10 approximately equal to  $2 \times 10^{18}$  atoms/ $\text{cm}^2 \cdot \text{s}$  at the electron beam location. Once the beam intensity,  $I_b$ , exceeds unity (in a.u.) the beam density is sufficient for electron diffraction measurements. Because all three of these condensable gases are noble species, one is tempted to look for some universal behavior. Thus normalizing to Xe, the three curves are replotted as dashed lines in terms of an abscissa equal to  $P_0 e/k$ , where  $e$  is the interatomic potential well depth<sup>5</sup> and  $k$  Boltzmann's constant. When plotted in this manner the onset of condensation occurs at the same value of  $P_0 e/k$  for the three gases.

A plot of these same data as a function of a nondimensional or reduced pressure  $P_0/(e/\sigma^3)$  or  $P_0/(e/\sigma^3)$ , where  $\sigma$  is the radius for zero interaction potential<sup>6</sup> and  $P_0$  is the condensable vapor partial pressure, did not unify the onset point.

For a given species and mole fraction, nucleation results from one nozzle to another will now be compared. Results for Ar,  $X_0 = 0.25$ , for Nozzles 11-13 are shown in Fig. 6. The solid lines are for the data plotted as a function of  $P_0$ . The onset of nucleation occurs first for the nozzles with the two largest diameters. Nozzle 12, with a lower expansion rate than Nozzle 11, exhibits a more rapid growth of the condensed phase after onset since the measured beam intensity beyond onset is due entirely to the condensed phase. As with free-jet cluster sources, these data have also been plotted vs  $P_0$  (dashed lines) such that the curve for Nozzle 12 is unchanged. Recall that  $P_0$  is proportional to the total number of binary collisions per atom for a given expansion. Here again it is interesting to note that detectable condensation onset occurs

at a single point on the  $P_0 D_0$  scale. Note, however, that the three curves would also converge to a common onset point were they plotted versus  $P_0^2 D_0$  which is proportional to the three-body collision frequency if this type of collision were required to form a stable dimer in the initial cluster formation process. These results, although interesting, are not universal, as seen in Fig. 7 for expansions with  $X_0$  and  $X_0 = 0.04$ . In this case the onset of nucleation in Nozzle 11 occurs at lower  $P_0$  than that of Nozzle 12, and their growth curves cross over at a higher pressure. When replotted versus  $P_0 D_0$  (dashed lines) the results from Nozzles 12 and 13 (which have the same nozzle contour but different  $D_0$ ) fall nicely on top of one another, whereas the results from Nozzle 11 move slightly away. Thus the correlation with binary or tri-molecular collision frequency is not perfect, but, of course, these various nozzle expansions do not have flow histories as universal as those of the free jet expansions.

#### Electron Diffraction

Electron diffraction patterns have been recorded with our single channel detection system for all three condensable noble gases under a variety of conditions and using several nozzles. An average cluster size can be estimated from the measured broadening of the diffraction rings in these patterns. Knowing the density of the condensed phase, the approximate number of atoms per cluster may then be calculated. Results for  $X_0$ ,  $X_0 = 0.04$  are shown in Fig. 8. These results fall in the  $g = 100-1000$  atoms per cluster range. There is a correlation of cluster size  $\bar{g}$  with beam intensity  $I_0$ , i.e., the higher the beam intensity the greater is the average cluster size. Also, to obtain a given value for  $I_0$  or  $g$  in the molecular beam, a higher  $P_0$  and thus higher mass flow rate, is required for Nozzle 13 than for Nozzle 12 and for Nozzle 12 than for Nozzle 11. Therefore, in order to provide a given beam intensity or cluster size, with the minimum mass flow rate, Nozzle 11 is the best of the three.

Theoretical models for the structure of noble gas clusters in this size regime predict the possibility of icosahedral packing in contrast to the bulk face-centered cubic (FCC) structure.<sup>9,10</sup> The comparisons we have made between data and cluster models have so far shown better agreement using icosahedral rather than the bulk structure. That is to say, the temperature of these clusters is low enough so that their diffraction patterns reveal a crystalline state in contrast to that of liquid, and that their structure is progressively more like icosahedral and less like bulk FCC as the cluster size is reduced.

#### Conclusions

We have arrived at the following conclusions with regard to noble gas clustering in small Laval nozzles:

- 1) Noble gases, even when expanded as a small mole fraction in helium, readily nucleate.
- 2) Because of the high kinematic viscosity of helium the nozzle contour must be carefully designed to balance the effects of increased boundary layer growth and the requirement that throat diameter be small enough to avoid pumping problems.
- 3) There is tantalizing evidence that a parameter  $P_0 D_0$  or  $P_0^2 D_0$  will provide correlation or scaling with regard to the onset of nucleation.
- 4) Cluster beam intensities (actually cluster densities) high enough to conduct electron diffraction can be attained in a size range of great interest for study of the structure of the condensed phase and possible deviations from the bulk-matter structure.

#### Acknowledgments

The authors would like to thank the Engineering Energetics section of the National Science Foundation and the Power Branch and the Chemistry Program of the Office of Naval Research for partial support of this work.

#### References

- 1) Hagena, O. F. and Obert, W., "Cluster Formation in Expanding Supersonic Jets: Effect of Pressure, Temperature, Nozzle Size, and Test Gas," *Journal of Chemical Physics*, Vol. 56, 1972, p. 1793.

<sup>2</sup>Tagawa, O. F., Molecular Beams and Low Density Gas Dynamics, edited by P. P. Wegener, Marcel Dekker, New York, 1974.

<sup>3</sup>DeBoer, B. G., Kim, S. S., and Stein, G. D., "Molecular Beam Studies of Sulfur Hexafluoride Clustering in an Argon Carrier Gas from Both Free Jet and Laval Nozzle Sources," High Speed Gas Dynamics, edited by R. Campargue, Commissariat A L'Energie Atomique, Paris, 1979, p. 1151.

<sup>4</sup>Obert, W., "Properties of Cluster Beams Formed with Supersonic Nozzles," High Speed Gas Dynamics, edited by R. Campargue, Commissariat A L'Energie Atomique, Paris, 1979, p. 1181.

<sup>5</sup>Abraham, O., Shim, J. H., DeBoer, B. G., and Stein, G. D., "Gas Dynamics of Very Small Laval Nozzles," to appear in Physics of Fluids, 1980.

<sup>6</sup>Boesel, U., "Investigation of Skimmer Interaction Influences on the Production of Aerodynamically Intensified Molecular Beams," Ph.D. thesis, Astronomical Sciences Division, Univ. of California, Berkeley, Calif., 1968.

<sup>7</sup>Armstrong, J. A., "An Investigation of the Physical Properties of Small Molecular Clusters Formed Via Homogeneous Nucleation in Nozzle Beams," Ph.D. thesis, Dept. of Mechanical Engineering and Astronomical Sciences, Northwestern University, Evanston, Ill., 1973.

<sup>8</sup>Mirschfelder, J. O., Curtiss, C. F., and Bird, E. B., Molecular Theory of Gases and Liquids, Table I-A, Wiley and Sons Inc., New York, 1964, pp. 1110-1111.

<sup>9</sup>Brient, G. L. and Burton, J. J., "Molecular Dynamics Study of the Structure and Thermodynamic Properties of Argon Micro-clusters," Journal of Chemical Physics, Vol. 63, 1975, p. 2045.

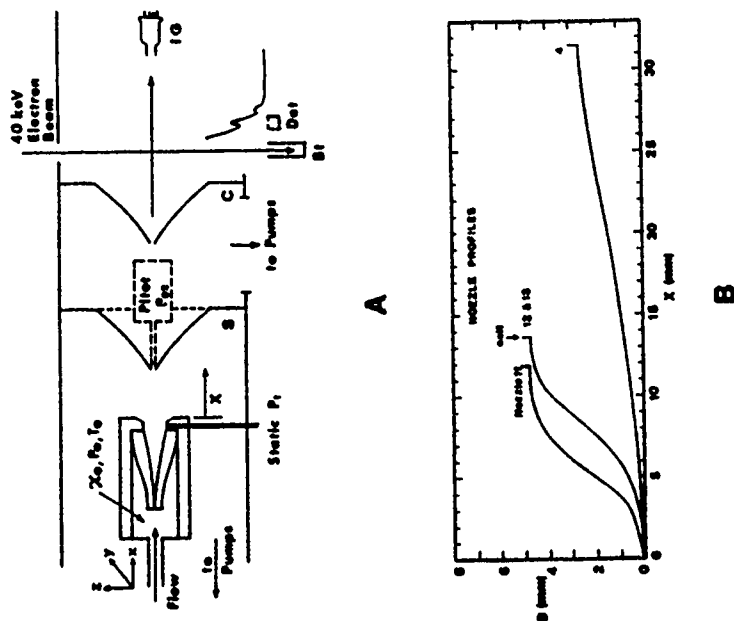


Fig. 1 The experimental arrangement shows the nozzle and stagnation chamber movable in xyz space with either a skimmer S or a pitot probe and transducer located downstream of the nozzle exit. With the skimmer and collimator C in place the resultant molecular beam is crossed with a 40 keV electron beam which is trapped in a beam trap Bt. Diffraction patterns are obtained with a detector Det. The nozzle contours are shown in Fig. 1b, with additional details given in Table I.

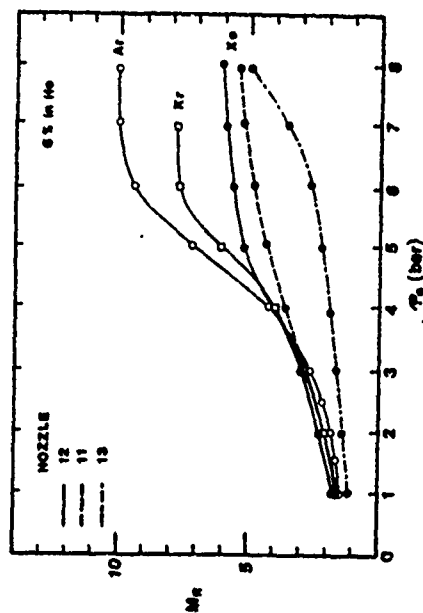


Fig. 2 Typical exit Mach numbers obtained using Eq. (1) are shown for Nozzle 12 as solid lines for Ar, Kr, and Xe, and as dashed lines for He in Nozzles 11 and 13. All expansions begin with  $T_0 \approx 295$  K and  $X_0 = 0.06$  in a He carrier gas.

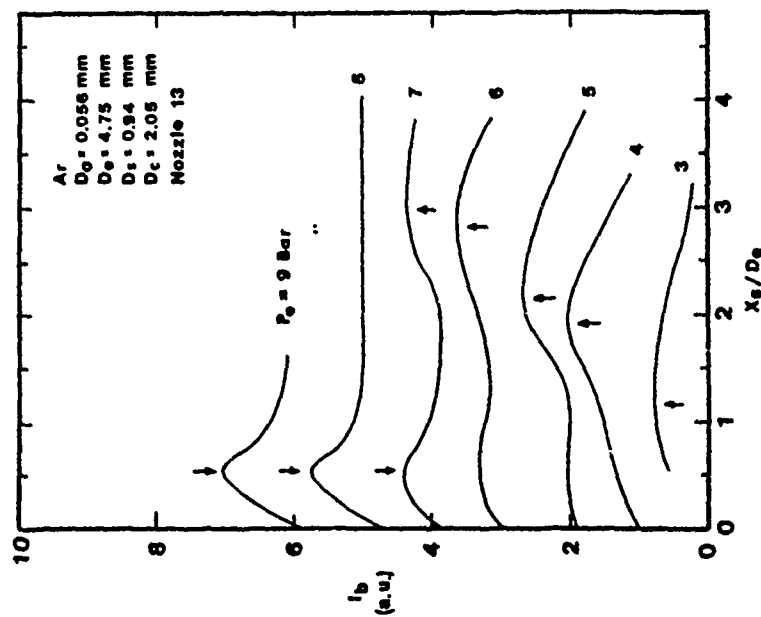


Fig. 3 Molecular beam intensities  $I_b$  as a function of distance from the nozzle exit to the skimmer. Locations of maximum beam intensity indicated by arrows.

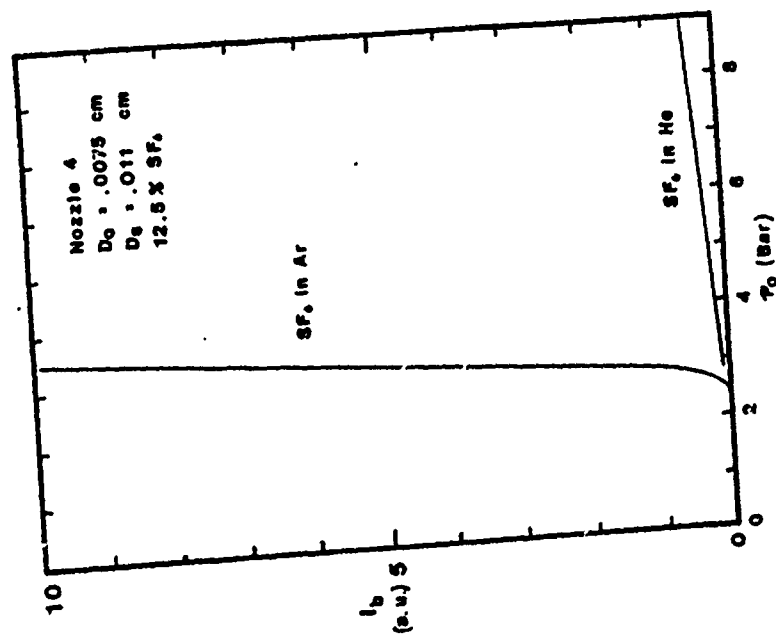


Fig. 4 Molecular beam intensities for  $\text{SF}_6$  for Nozzle 4 with Ar and He carrier gases.

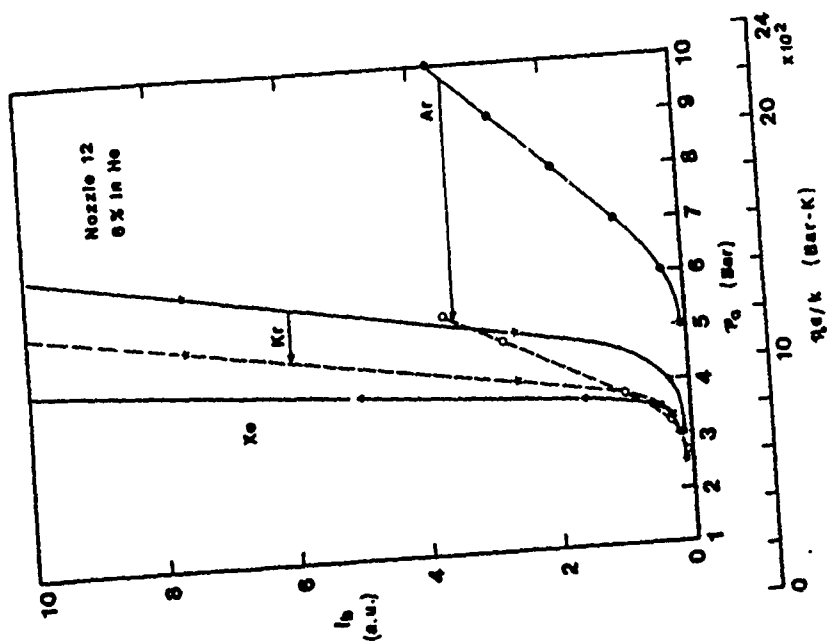


Fig. 5 Beam intensities as a function of  $P_0$  (solid lines) for Nozzle 12 with  $X_0 = 0.06$  and a He carrier gas. With a scale change to  $P_0$  pc/K, the curves for Ar and Kr move to the dashed lines as indicated by the arrows.



<sup>10</sup> Farges, J., deFerdudy, M. P., Racot, B., and Torchet, G., "Structure Compacte Déformable et Agrégats Moléculaires Modèles Polycycliques." *Journal de Physique Colloque C2*, Vol. 36, 1975, pp. C2-13.

Table I. Nozzle Geometry<sup>a)</sup>

Nozzle Number	4	11	12	13
$P_0$ -cm	0.0063	0.0099	0.0089	0.0056
$D_0$ -cm	0.256	0.47	0.47	0.47
$L$ -cm	3.15	1.176	1.356	1.283
$a_0$	0.00635	0.0088	0.009	0.0053
$a_1$	-0.0248	-0.0150	0.0150	-0.1402
$a_2$	0.1488	4.6518	-1.6208	2.473
$a_3$	-0.1156	-43.562	23.052	-13.2382
$a_4$	0.0450	+180.334	-120.408	39.238
$a_5$	-0.00637	-381.34	337.06	-63.936
$a_6$	0	+378.88	-561.0	59.626
$a_7$	0	-201.50	579.44	-29.726
$a_8$	0	43.0.-	-366	6.0812
$a_9$	0	0	129.404	0
$a_{10}$	0	0	-19.6	0

<sup>a)</sup> A best fit polynomial equation of the form,

$$D(X) = \sum_{i=0}^{10} a_i X^i$$

is fitted to measured contours, with D and X in cm.

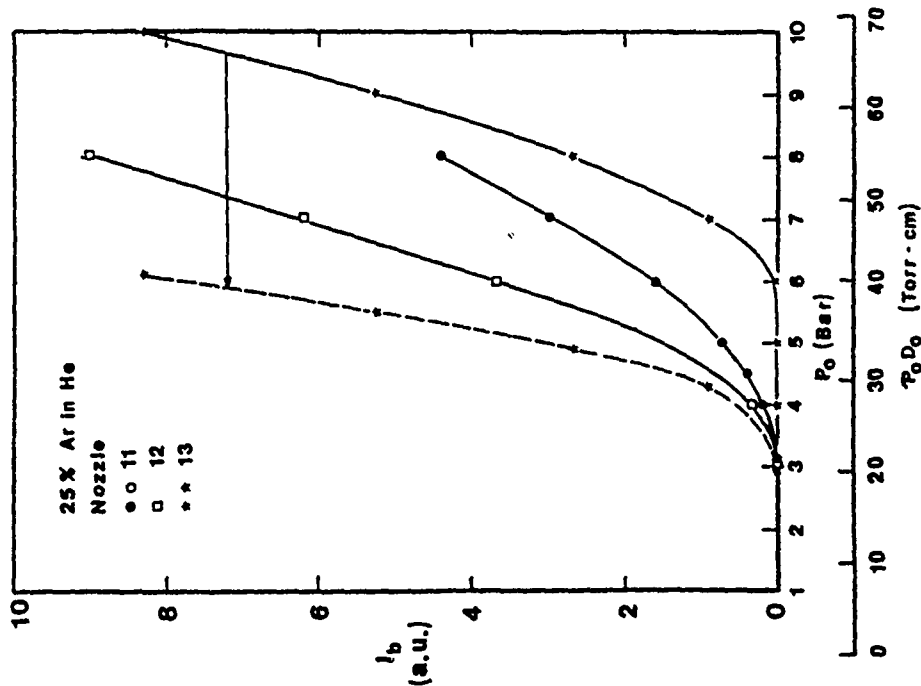


Fig. 6 Beam intensities as a function of  $P_0$  (solid lines) and  $P_0 D_0$  normalized to Nozzle 12 (dashed lines) for Ar,  $X_0 = 0.25$  in a He carrier gas.

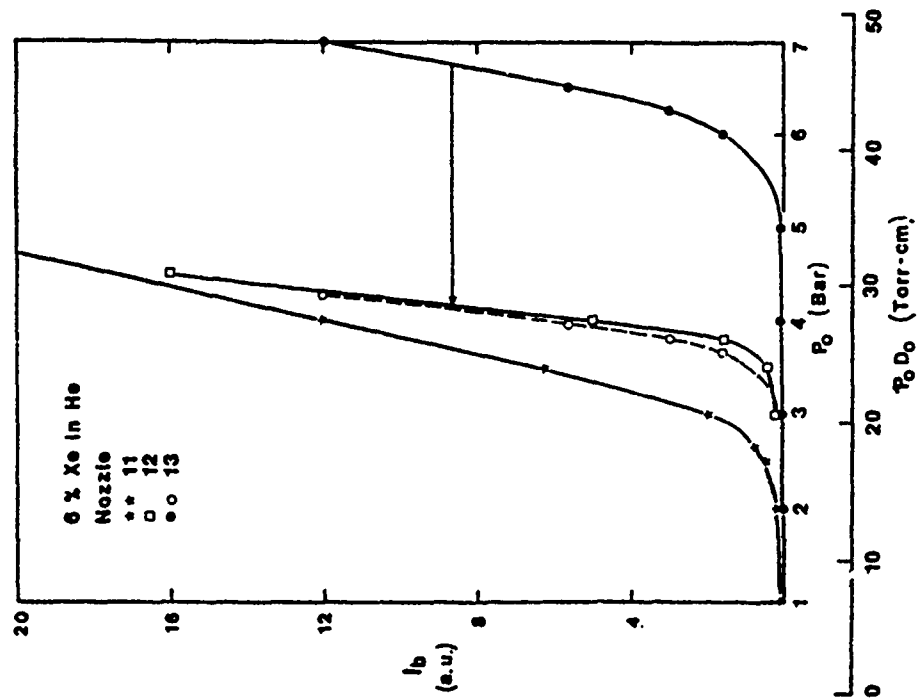


Fig. 7 Beam intensities as a function of  $P_0$  (solid lines) and for the ordinate  $P_0 D_0$  normalized to Nozzle 12 (dashed curves) for Xe,  $X_0 = 0.06$  in a He carrier gas.

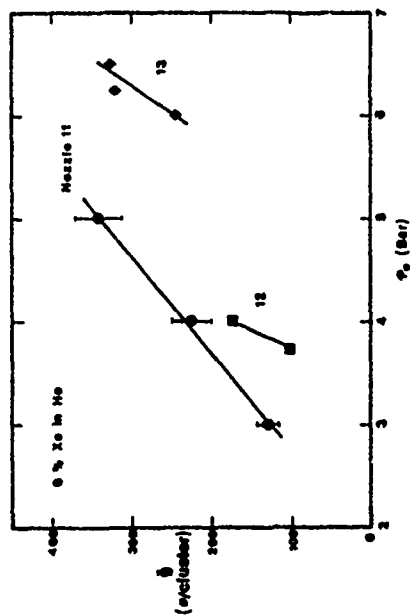


Fig. 8 The average number of atoms per cluster  $\bar{n}$  versus  $P_0$  for Xe,  $X_0 = 0.06$  in a He carrier gas for Nozzles 11-13.